Comparing Fuzzy and Intelligent PI Controllers in Stop-and-Go Manoeuvres

Vicente Milanés, Jorge Villagrá, Jorge Godoy, and Carlos González

***Abstract*—The aim of this work was twofold: on the one hand, to describe a comparative study of two intelligent control techniques—fuzzy and intelligent proportional-integral (PI) control, and on the other, to try to provide an answer to an as yet unsolved topic in the automotive sector—stop-and-go control in urban environments at very low speeds. Commercial vehicles exhibit nonlinear behavior and therefore constitute an excellent platform on which to check the controllers. This paper describes the design, tuning, and evaluation of the controllers performing actions on the longitudinal control of a car—the throttle and brake pedals—to accomplish stop-and-go manoeuvres. They are tested in two steps. First, a simulation model is used to design and tune the controllers, and second, these controllers are implemented in the commercial vehicle—which has automatic driving capabilities—to check their behavior. A stop-and-go manoeuvre is implemented with the two control techniques using two cooperating vehicles.**

***Index Terms*—Fuzzy control, intelligent control, nonlinear control, proportional-integral-derivative (PID), road vehicles.**

I. Introduction

SAFETY is crucial in the development of autonomous systems in the transportation research field, with both manufacturers and research groups focusing efforts in this direction. The aim is to develop advanced driver assistance systems (ADAS) that will increase safety in carrying out driving-related tasks. The first system introduced in commercial vehicles with the potential to influence traffic safety and traffic flow characteristics was adaptive cruise control (ACC) [1], [2].

ACC is an extension of cruise control (CC)—CC allows the driver to set a driving speed—in which the vehicle is capable of following a leading car on highways by actions on the throttle pedal. These commercial systems work at speeds greater than 30 km/h. Their main drawback is that they are useless in urban environments.

Recently, commercial systems capable of stopping the vehicle when a collision is imminent at speeds below 15 km/h have been developed by car manufacturers, but their dependence on the human driver to restart the vehicle might cause traffic jams. Thus, autonomous intelligent driving in traffic jam conditions is one of the most challenging topics of large city traffic management. These kinds of system are known in the literature as stop-and-go systems [3]. They deal with the vehicle in urban scenarios with frequent and sometimes hard braking and acceleration. The main idea of these control systems is to regulate the vehicle around the well-known 2-s headway rule, which attempts to maintain a distance proportional to the human reaction time (approximately 2 s) [4]. Some approaches have tried to reproduce human behavior with deterministic models in order to achieve smooth control actions. Unfortunately, this kind of strategy may not necessarily lead to safe operation.

In [5], Martinez and de Wit proposed a nonlinear reference model taking into account safety and comfort specifications in an intuitive way. However, their approach assumes that the reference acceleration generated by the dynamic inter-distance (or gap-distance) model is applied instantaneously to the following vehicle. Since this assumption is hardly ever satisfied in real urban situations, an advanced feedback controller should be introduced to cope with vehicle nonlinearities—especially in brake and engine dynamics at low speed—and environmental disturbances.

Different approaches have been proposed to tackle the actuators' nonlinear dynamics. Input/output linearization [6], fuzzy logic [7], [8], and sliding mode control [9], [10] have been used to deal with engine control. Feedback linearization [11] and sliding modes [12] have also been implemented to control a nonlinear brake model. However, most of these approaches require precise models, so that any parameter variation during the vehicle's lifetime may lead to deteriorating performance, or even to unstable behavior. The present work is an attempt to find an engine/brake control algorithm that yields the expected reference speed and acceleration of the trailing vehicle, while keeping a reference distance from the leading vehicle. Moreover, the control law will have to be robust to measurement noise, unmodeled (brake and engine) dynamics and disturbances (road inclination, aerodynamic forces, and rolling resistance).

To that end, two control techniques will be implemented and compared both in simulation and in a commercial vehicle: fuzzy logic and an intelligent proportional integral (PI) controller.

The first of these is one of the class of soft computing techniques [13]. These techniques are recognized as having a strong learning and cognition capability as well as good tolerance to uncertainty and imprecision. Among them, fuzzy logic—developed by Prof. L. A. Zadeh in 1965 [14]—gives a good approximation to human reasoning, and hence provides an intuitive approach to autonomous control of the nonlinear behavior of commercial vehicles [15].

The second control algorithm uses a novel technique that, based on the classical PI controller structure, is capable of dealing with parameter uncertainties and unmodeled nonlinear dynamics. This control paradigm [16], [17] replaces physical

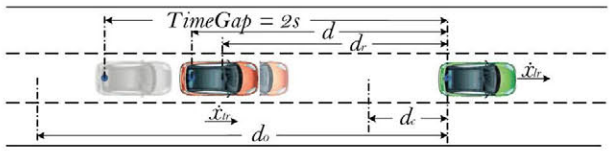

Fig. 1. Stop-and-Go scheme.

models by local input/output differential equations, valid over short lapses of time. The main advantage of this new approach is that these phenomenological models are merged into a PI transparently, so that an "intelligent" (hence the name i-PI) term compensates the effects of poorly-known dynamics.

In brief, the following issues will be tackled in the present communication.

- Design and development of two valid solutions for an as yet unresolved issue in the automotive sector: ACC in urban environments at very low speeds.
- A comparative study of these intelligent control techniques, examining their robustness via a Monte Carlo analysis.
- Comparison with previously presented solutions [5] to this problem to illustrate the improvements contributed by the present work.
- Implementation in a commercial car—a convertible Citroën C3 Pluriel with automated brake and throttle—to validate the controllers in a real environment.

The rest of this brief is organized as follows. The second section will be devoted to briefly presenting the dynamic inter-distance and relative velocity model. In Section III, the design and tuning of the controllers will be presented using a vehicle model. Then the fuzzy and the i-PI controllers will be detailed. Finally, a test of the controllers in a simulation environment will be described, using a Monte Carlo analysis to assess the system's robustness. In Section IV, the two control techniques will be evaluated and compared to a classical PI controller on a real experimental platform, with a focus on comfort and safety aspects. Finally, Section V will present some concluding remarks and a description of future work in this line.

II. Generation of the Reference Inter-Distance and Relative Velocity

As mentioned above, the goal of the control strategies will be to use the throttle and brake (control variables u_e and u_b, respectively) to track as precisely as possible a reference distance between vehicles d_r and a target relative velocity v_r. A reference model proposed by [5] will provide these two variables, and the ideal acceleration $\ddot{x}_{t_r}$ the trailing car should have to follow the trajectories of those two reference variables.

Note in Fig. 1 that d_r is related to the safe nominal inter-distance d_0—the maximum distance at which the control algorithm will be activated—and the critical distance d_c—the minimum distance between cars which is only attained when they are stopped. Note also that the dynamic reference model used in the present work will provide a reference inter-distance less than the 2-s headway rule if the allowed maximum acceleration is high enough (for more details, see Fig. 2).

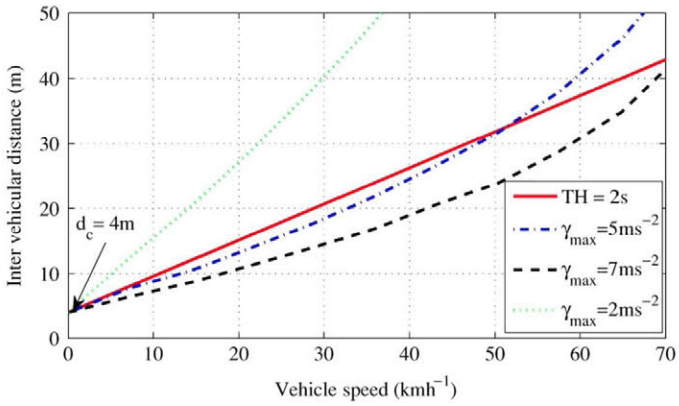

Fig. 2. Comparison of different distance policies: constant headway rule (2 s) and the inter-distance model [5] with different maximum accelerations.

The inter-distance reference model describes the virtual dynamics of a vehicle which is positioned at a distance d_r (the reference distance) from the leading vehicle

$$\ddot{\tilde{d}}_r = \ddot{x}_l - \ddot{x}_{t_r} \tag{1}$$

where $\ddot{x}_l$ is the leading vehicle's acceleration and

$$\ddot{x}_{t_r} = u_r(d_r, \dot{d}_r) \tag{2}$$

is the trailing acceleration, which is a nonlinear function of the inter-distance and its temporal derivative.

Considering $\tilde{d} = d_0 - d_r$ in (2), where d_0 is the safe nominal inter-distance, the control problem is then to find a suitable trailing car acceleration u_r, when $\tilde{d} \geq 0$, such that all the solutions of (1) satisfy the following comfort and safety constraints:

- $d_r \geqslant d_c$, with d_c the minimal inter-distance;
- $|\ddot{x}_r| \leqslant \gamma_{\max}$, where $\gamma_{\max}$ is the maximum attainable longitudinal acceleration;
- $|\dddot{x}_r| \leqslant J_{\max}$, with $J_{\max}$ a driver desired bound on the jerk.

Martinez and de Wit [5] propose the use of a nonlinear damping model $u_r = -c|\tilde{d}|\dot{\tilde{d}}$—where c plays the role of a damping constant—which can be introduced into (1) to give

$$\ddot{\tilde{d}} = -c|\tilde{d}|\dot{\tilde{d}} - \ddot{x}_l.$$

This equation can be integrated analytically and expressed in terms of d_r as follows:

$$\dot{d}_r = \frac{c}{2}(d_0 - d_r)^2 + \dot{x}_l(t) - \beta,$$
$$\beta = \dot{x}_{t_r}(0) + \frac{c}{2}(d_0 - d_r(0))^2. \tag{3}$$

Note that this reference speed depends upon the leading vehicle's speed, the distance d_0, and the parameter c, which is in turn an algebraic function of the safety and comfort parameters d_c, $V_{\max}$, $\gamma_{\max}$, and $J_{\max}$ [5]. Fig. 2 shows how $\gamma_{\max}$ influences the reference inter-vehicle distance.

Finally, from (2) the trailing acceleration is

$$\ddot{x}_{t_r} = u_r = c|d_0 - d_r|\dot{d}_r \tag{4}$$

where the inter-distance evolution is given by the numerical integration of (3).

Once the reference inter-distance and its time derivative (d_r and $v_r = \dot{d}_r$, respectively) have been generated, the fuzzy and i-PI controllers will seek to ensure that these two variables are tracked as closely as possible.

III. Design and Tuning of the Controllers

To design the controllers, a vehicle model was developed which includes the vehicle's dynamics at very low speeds so as to constitute a good starting point in tuning the controllers. This section briefly describes the model and the design of each of the controllers, a simulation comparing the controllers before their implementation in a real car, and finally Monte Carlo simulations to analyze the robustness to disturbances or parameter uncertainties.

A. Vehicle Model

The balance of forces along the vehicle's longitudinal axis [18] is

$$M\dot{V}_x = F_{x_f} + F_{x_r} - F_a - R_{x_f} - R_{x_r} - Mg\sin\theta \qquad (5)$$

where M is the mass of the vehicle, V_x the longitudinal velocity, F_{x_f} and F_{x_r} the front and rear longitudinal tyre forces, respectively, R_{x_f} and R_{x_r} the front and rear tyre forces due to rolling resistance, θ the angle of inclination of the road, and F_a the longitudinal aerodynamic drag.

The rolling resistance forces are often modeled as linear functions of the normal forces on each tyre, i.e., $R_x = k_r F_z$, with k_r the rolling resistance coefficient and F_z the vertical load of the vehicle. The aerodynamic forces can be expressed as

$$F_a = \frac{1}{2}\rho C_d A_F (V_x + V_{\text{wind}})^2$$

with ρ being the mass density of air, C_d the aerodynamic drag coefficient, A_F the frontal area of the vehicle (the projected area of the vehicle in the direction of travel), and V_{wind} the wind speed. The Pacejka model [19] is used for longitudinal tyre/road interaction forces F_x.

The rotation dynamics of each wheel can be expressed as

$$I\dot{\omega}_i = -rF_{x_i} + \tau_{e_i} - \tau_{b_i} \qquad (6)$$

where I is the wheel's moment of inertia, $\dot{\omega}_i$ the angular velocity of each wheel, r the tyre radius, τ_{e_i} the applied engine torque, and τ_{b_i} the brake torque, both applied to each wheel's center.

The total engine torque τ_e can be expressed in terms of the throttle opening u_e by the expression [20]

$$\tau_e = n u_e \tau_m \left(1 - \beta_m \left(\frac{\omega}{\omega_m} - 1\right)^2\right)$$

where n is the gear ratio, ω is the average wheel speed, β_m is an engine torque parameter, and the maximum torque τ_m is obtained at engine speed ω_m.

Finally, the dynamics between the braking control variable u_b and braking torque τ_b can be modeled as a second-order linear system

$$\tau_b(s) = \frac{K_b}{s^2 + 2\eta_b\omega_b s + \omega_b^2} u_b(s)$$

TABLE I
Model Parameters

Parameter	Nominal Value
M	1418
C_d	0.32
A_F	2.4
C_x	40000
r	0.21
I	2
n	25
τ_m	190
β_m	0.4
ω_m	420
K_b	220
η_b	0.45
ω_b	1023

with K_b, η_b, and ω_b being the static gain, damping factor, and natural frequency, respectively. Since the braking dynamics is much faster than that of the vehicle, it can be replaced in the vehicle model by an algebraic expression, without loss of realism [21]. The numerical values of the model parameters are given in Table I.

B. Fuzzy Controller

Fuzzy logic was selected as one of the control techniques to compare because it is a well-tested method for dealing with this kind of system, yields good results, and can incorporate human procedural knowledge into the control algorithms [22]. Also, it allows the designer to partially mimic human driving behavior.

The rationale behind the design of the fuzzy controller is to select two errors—distance and speed—as inputs so that the controller can emulate the behavior of a human driver who, in this situation, would control these two parameters. To this end, for each fuzzy variable a central membership function is introduced to define an area of good performance. Two further membership functions are defined to represent the higher and lower error regions with respect to the target reference. In this sense, to keep a reference distance, a driver does the following:

- presses the throttle if the distance is greater than the reference distance;
- presses the brake if the distance is less than the reference distance;
- lifts the pedal foot off the pedals if the distance is correct.

These will also be the actions of our controller since it will try to mimic human behavior.

The membership function definition for each of the input variables are shown Fig. 3. The two variables used to perform the control are the *SpeedError*, defined as the difference between the desired relative velocity between the leading and trailing car and its actual value ($\dot{d}_r - (\dot{x}_l - \dot{x}_t)$), and the *DistanceError*, defined as the difference between the optimal distance determined using the dynamic inter-distance model generator and the real distance between cars ($d_r - (x_l - x_t)$). Obviously the goal of our controller is to perform actions maintaining the values of these two variables close to zero.

The choice of the membership functions of each input variable is based on expert drivers' experience. In this sense, the goal of our approach to stop-and-go scenarios is based on following both a reference distance and a reference relative velocity. One can easily adjust the fuzzy controller for this purpose

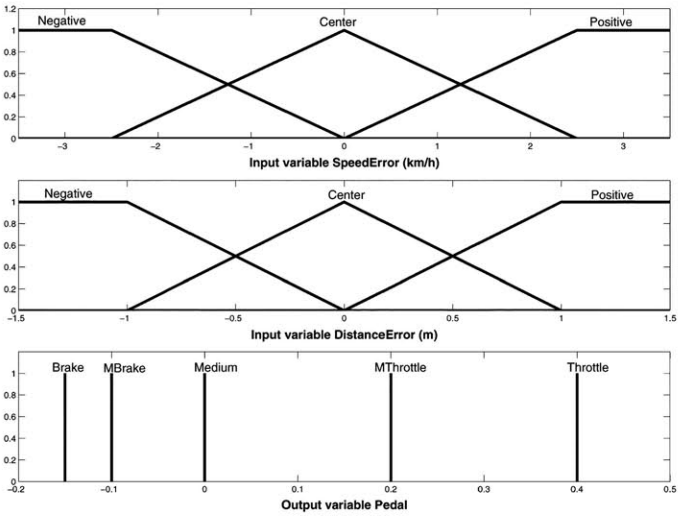

Fig. 3. Membership functions.

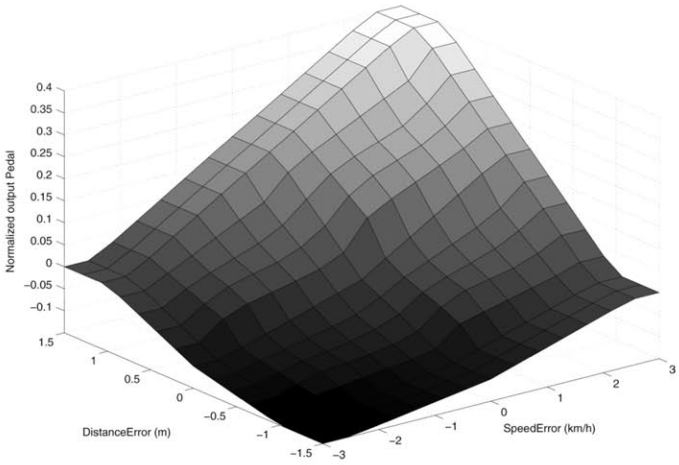

Fig. 4. Speed control surface.

by defining errors of these values with respect to actual values obtained from the vehicle's sensors. For tuning, simulation with the car model is used to adjust the membership functions to the actual vehicle that will subsequently be used in the experimental phase. The controller can be easily readjusted to suit any kind of vehicle by slightly modifying the membership functions, in particular, by searching for the optimal tradeoff between good reference tracking and smooth control actions.

The output generated is the action on the longitudinal actuators—i.e., throttle and brake pedals. In particular, the fuzzy output variable *Pedal* determines which actuator has to be pressed, and the magnitude of the action. The shape of its membership function is defined in terms of Sugeno singletons. The possible output values lie within the range $[-1, 1]$, where -1 indicates the brake pedal u_b is completely depressed and 1 indicates the maximum action is applied to the accelerator pedal u_e. In the present case, these values will be less than unity since the controller will be used at very low speeds (see the bottom plot in Fig. 3). Fig. 4 shows the control surface for the output variable as a function of the input variables of our fuzzy controller. The output values assigned for each rule are listed in Table II.

TABLE II
RULE BASE

	DistanceError		
SpeedError	*Negative*	*Center*	*Positive*
Negative	Brake	MBrake	Medium
Centre	MBrake	Medium	MThrottle
Positive	Medium	MThrottle	Throttle

C. i-PI Controller

Intelligent PI controllers are used in this work because they combine the well-known PI structure with an "intelligent" term that compensates the effects of nonlinear dynamics, disturbances, or uncertainties in the parameters. As a consequence, the nonlinear dynamics of the car at low speeds become controllable with this novel technique.

Following [17], [23], a finite-dimensional nonlinear system can be written locally as

$$y^{(\mu)} = F + \alpha u \tag{7}$$

where $\alpha \in \mathbb{R}$ and $\mu \in \mathbb{N}$ are two constant parameters, which do not necessarily represent physical magnitudes, and whose choice is based on the following guidelines:

- μ is usually 1 or 2, and may, although not necessarily, represent the system order.
- α should allow F and αu to be of the same order of magnitude.

The term F, which is a sort of nonlinear black box identifier [17], is computed from the input value at the preceding sample time $u(t_{k-1})$ and the μth derivative estimate of the output $\hat{y}^{(\mu)}(t_k)$ at the current sample time

$$F(t_k) = \hat{y}^{(\mu)}(t_k) - \alpha u(t_{k-1}). \tag{8}$$

Using the formalism introduced in (7) and (5) for the two vehicles, the relative velocity dynamics can be expressed as

$$\ddot{x}_{t_r}(t) = F(t) + \alpha u(t) \tag{9}$$

where $u = \{u_e, u_b\}$ are respectively the engine and brake control variables.

If (9) is inverted and merged with a PI controller [20], the resulting i-PI control law is

$$\begin{aligned} u &= \frac{1}{\alpha}(\ddot{x}_{t_r} - F) + K_P e + K_I \int e dt, \\ e &= \dot{d}_r - (\dot{x}_l - \dot{x}_t) \end{aligned} \tag{10}$$

where K_P, $K_I \in \mathbb{R}^+$ are PI gains. Even though this system is nonlinear and has varying parameters, the linearized model of (5) can be useful to tune the PI controller classically (see [20]).

Two extra parameters α_e and α_b are chosen (see Table III) to enhance the dynamic behavior and disturbance rejection of the

TABLE III
CONTROL PARAMETERS

Controller	$\mathbf{K_{p_e}}$	$\mathbf{K_{i_e}}$	$\alpha_\mathbf{e}$	$\mathbf{K_{p_b}}$	$\mathbf{K_{i_b}}$	$\alpha_\mathbf{b}$
PI	0.203	0.243	–	0.277	0.146	–
i-PI	0.203	0.243	30	0.277	0.146	40

closed-loop system, particularizing (10) in our case to control the throttle

$$\begin{aligned} u_e(t_k) &= \frac{1}{\alpha_e}(\ddot{x}_{t_r}(t_k) - F_e(t_k)) + K_{p_e} e(t_k) \\ &\quad + K_{i_e} \int (e(t_k))dt \\ F_e(t_k) &= \hat{\ddot{x}}_t(t_k) - \alpha_e u_e(t_{k-1}) \end{aligned} \tag{11}$$

and to do likewise with the brake

$$\begin{aligned} u_b(t_k) &= \frac{1}{\alpha_b}(\ddot{x}_{t_r}(t_k) - F_b(t_k)) + K_{p_b} e(t_k) \\ &\quad + K_{i_b} \int (e(t_k))dt \\ F_b(t_k) &= \hat{\ddot{x}}_t(t_k) - \alpha_b u_b(t_{k-1}) \end{aligned} \tag{12}$$

where $\hat{\ddot{x}}_t$ is a velocity derivative estimate. Since measurements of the acceleration are available from the CAN bus, this second derivative estimate will not be necessary in this case.

Finally, a decision rule will be established to determine whether brake or throttle actions are needed. The control law (12) will be triggered if the reference acceleration is negative and the inter-distance error is less than a fixed value ϵ. In any other case, the throttle control law (11) will be used. The resulting control law turns the automated vehicle into a nonlinear hybrid system. It is well known how difficult it is to assess the stability of such complex systems. However, a recent work addressing this issue [24] has demonstrated the generalized applicability of this kind of controller to such hybrid systems

$$u_e = \begin{cases} 0, & \text{if } \ddot{x}_{t_r} < 0 \wedge |d_r - (x_l - x_t)| < \epsilon \\ \text{Eq. (11)}, & \text{otherwise} \end{cases}$$

$$u_b = \begin{cases} \text{Eq. (12)}, & \text{if } \ddot{x}_{t_r} < 0 \wedge |d_r - (x_l - x_t)| < \epsilon \\ 0, & \text{otherwise.} \end{cases}$$

1) Tuning Procedure: To evaluate the closed-loop system's behavior with the two controllers, the vehicle's dynamics will be simulated, as mentioned above, with a realistic model which takes into account tyres, brakes, and engine dynamics. Measurement noise in the velocity and acceleration CAN-based sensors will also be considered. These corrupting noises will be modeled as additive white Gaussian variables [see the inset in Fig. 6(a)]. The value taken for the transmission rate will be 5 Hz, set by the GPS receiver as detailed in Section IV-A.

Fig. 5 shows a velocity profile plot for the leading vehicle. The idea behind this scenario was to evaluate the control algorithms over a wide operating range, trying to emulate coping with the most demanding manoeuvres in urban driving conditions. A robust longitudinal control algorithm [25] will be applied to the first car to track the setpoints as precisely as possible. Furthermore, both the leading and the trailing cars will have to

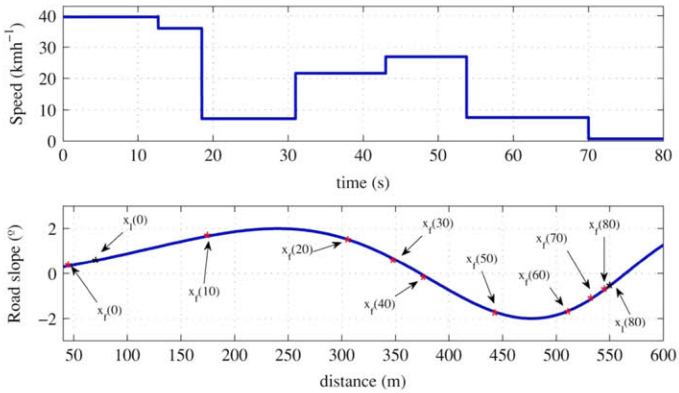

Fig. 5. Leading vehicle speed and road slope profiles.

accomplish their control goals while rejecting disturbances induced by the slope of the roadway depicted in Fig. 5.

The leading and trailing cars will initially be separated by a distance of 49 m and running at the same speed, $\dot{x}_l = \dot{x}_t = 11$ ms^{-1}. The inter-distance dynamic model is parameterized to provide a maximum speed $V_{\max} = 50$ km/h^{-1}, a maximum acceleration $\gamma_{\max} = 2$ ms^{-2}, a maximum jerk $J_{\max} = 5$ ms^{-3}, and a minimum inter-distance $d_c = 6$ m.

The controllers will be quantitatively tuned and evaluated with respect to an optimization criterion. Several fitness functions are commonly used to tune PI controllers. Among them, the integral absolute error (IAE) is the best adapted to our situation because of its sensitivity. Thus, a cost function including the distance error, the speed error, and the control action's smoothness will be used to design our PID-based controllers

$$J = \frac{1}{T}\int_0^T (|e_p| + |e_v| + u_s)dt$$

where $e_p = d_r - (x_l - x_t)$ is the distance tracking error, $e_v = v_r - (\dot{x}_l - \dot{x}_t)$ is the relative velocity error, and $u_s = |(du_e(t))/(dt)| + |(du_b(t))/(dt)|$ measures the control smoothness. The sum of engine and brake control variables u_e and u_b is equivalent to the *Pedal* variable in the fuzzy control implementation.

The optimization process gives as a result the PI parameters listed in Table III. Note that i-PI parameters are chosen such that PI gains are the same than for the optimal PI controller and the α parameter, for both brake and throttle, was manually tuned thereafter.

D. Simulation Results

The evolution of the vehicles' speeds, the distance between them, the error with respect to the dynamic inter-distance model, acceleration, jerk, and the control action are shown in Fig. 6, which thus provides a synthesis of the most important aspects of the controllers' behavior. In this figure and henceforth, the dash-dotted red line will be used to correspond to the fuzzy controller, the dashed green line to the i-PI controller, and the solid blue line to the PI controller.

One appreciates that the PI controller presents the poorest behavior. With respect to the i-PI and fuzzy controllers, at first sight their behavior is satisfactory, but there are some important

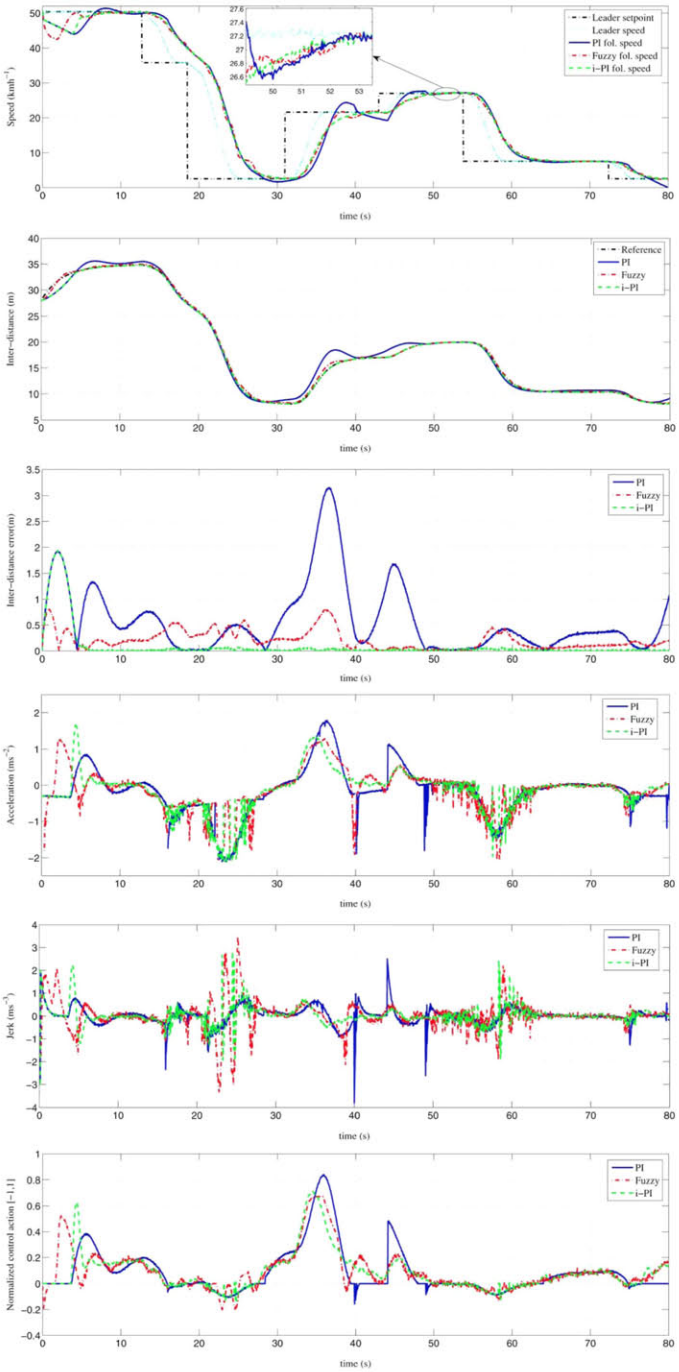

Fig. 6. (a) Leading and trailing vehicle speeds. (b) Inter-vehicular distance. (c) Inter-distance error. (d) Acceleration. (e) Jerk. (f) Normalized control action.

differences in terms of safety, comfort, and rejection of disturbances.

Concerning the inter-distance error relative to the dynamic reference, all the controllers present an initial transient that is corrected after approximately 5 seconds. From then on, i-PI provides more precise tracking than the fuzzy controller (see Table IV). Even though the fuzzy controller's tracking quality is not as good as i-PI's, the vehicle rarely exceeds the safe reference distance. The PI controller presents the worst behaviour, with inter-distance errors greater than 3 m. Also the values of the comfort indicator in Table IV—which shows that the i-PI's control action is smoother than the fuzzy controller's—is coherent with the fluctuating behavior of the fuzzy controller observed in the bottom plot of Fig. 6. Both the acceleration and the jerk constraints ($\gamma_{\max} = 2$ ms^{-2}, $J_{\max} = 5$ ms^{-3}) are satisfied by all three controllers.

TABLE IV
SIMULATION PERFORMANCE CRITERIA

IAE	PI	i-PI	Fuzzy
e_p	0.5858	0.0899	0.2086
e_v	0.2522	0.0619	0.1187
u_s	0.233	0.2905	0.5892
J	1.071	0.4423	0.9165

E. Robustness Analysis

Since no parameters appear explicitly in the closed form controller, classical robust control tools cannot here be exploited to analyze the closed loop system's sensitivity to disturbances or to parameter uncertainty. Non-deterministic techniques, in particular Monte Carlo methods, seem to be the most suitable tool to test robustness when model-free control laws are used.

To account for parameter uncertainty, we define the model's parameters as distributions of values rather than as single fixed values. We then perform a Monte Carlo simulation, running the model repeatedly with 1000 random combinations of parameter values. The parameters p_i in Table I will be considered to follow centred normal distributions of the form $\mathcal{N}(\mu_i, \sigma_i)$, $\mu_i = p_i, \sigma_i = 0.1\ \mu_i$. The amplitudes and frequencies of disturbances due to sinusoidal slopes are defined as uniform distributions between their maximum and minimum values ($[0.1\ \mu_i, 10\ \mu_i]$) to ensure that a wide design space is covered.

Table V summarizes the Monte Carlo results. One observes that all the implemented controllers are stable within the predefined uncertainty domain. However, there are significant differences between the three approaches. The smoothest action is provided by the PI controller. But with a slightly greater control action activity i-PI tracks distance and relative velocity much better than the optimized PI controller. The fuzzy controller also yields good tracking under the nominal conditions (see Table IV), but is more sensitive to disturbances and parameter uncertainty than the i-PI control law.

Fig. 7 shows the inter-distance and speed errors in the worst case for all three control strategies. One observes that both the fuzzy and the i-PI controllers improve the inter-distance and relative velocity tracking results obtained with the optimized PI. It also confirms that i-PI's behavior is remarkably good for both distance and relative velocity.

IV. EVALUATION OF THE CONTROLLERS

To validate the proposed control algorithms, the two controllers were implemented in the AUTOPIA program control architecture for autonomous vehicles [26]. This section presents a brief description of the real cars used for the experimental phase and their automation process. Then the real results at the CAR's facilities will be described.

TABLE V
MONTE CARLO ROBUSTNESS ANALYSIS

Controller	Distance error			Speed error			Control smoothness			Total		
	Mean	Std	Max	Mean	Std	Max	Mean	Std	Max	Mean	Std	Max
PI	0.6552	1.2742	21.9283	0.2514	0.0857	2.7353	0.2324	0.0246	0.3833	1.1052	0.7475	23.6856
i-PI	0.0893	0.0118	0.1282	0.0625	0.0052	0.0837	0.3870	0.1437	1.6215	0.5388	0.1514	1.7754
Fuzzy	0.4620	1.5816	35.6460	0.1568	0.0991	1.9259	0.6739	0.2654	4.7409	1.1359	1.5792	35.9256

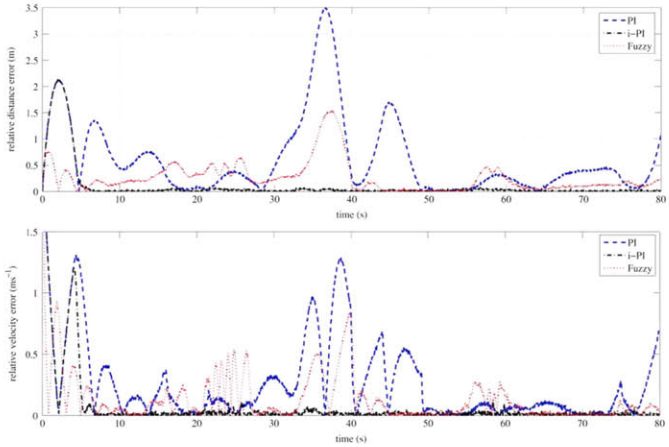

Fig. 7. Worst case in Monte Carlo simulations for all three controllers. (a) Position error. (b) Speed error.

Fig. 8. Commercial prototype vehicles used for the experimental phase.

A. Experimental Vehicles

Two vehicles were used for the experimental phase: a fully-automated vehicle and a manually driven one. The former is a convertible Citroën C3 Pluriel (see Fig. 8). The car is equipped with automatic driving capabilities with hardware modifications made to the throttle and the brake pedal actions. The latter vehicle is an electric Citroën Berlingo van (see Fig. 8) also equipped with automatic driving capabilities. For the purpose of this work, it was driven by a human driver making the leading car's behavior as close to a real traffic situation as possible.

With respect to the automation process, the Pluriel's throttle is controlled by an analogue signal that represents the pressure on the pedal, generated with an analogue card [27]. For the brake, an electro-hydraulic braking system is mounted in parallel with the original one [28], and is controlled via an I/O digital-analogue CAN card.

Both vehicles are equipped with real time kinematic—differential global positioning systems (RTK-DGPS) working at 5 Hz as the main sensor. This sensor is used to acquire driving information, providing 1-cm precision. An inertial measurement unit (IMU) is installed in the convertible car to provide positioning in case of GPS receiver failure [29]. A Personal Computer Memory Card International Association (PCMCIA) Proxim Wireless ComboCard is installed in the PC of each car, and a central station is used to send the relevant information from the leading to the trailing car [30]. The trailing vehicle is equipped with an industrial on-board PC that is in charge of receiving the information coming from the wireless communication system and the sensorial inputs, and of sending the output generated to the actuators in each control cycle (200 ms).

Remark 1: The system has been tested using DGPS in place of RTK-DGPS receivers, without degradation of performance. This kind of receiver removes the dependence on a local station to transmit the differential corrections, so that the system can work over hundreds of kilometers. Trials with low-cost commercial GPS receivers showed that they are as yet inappropriate for this kind of application.

B. Real Results

Several trials were conducted at the CAR's private driving circuit using the experimental vehicles. This circuit represents an inner-city area, with a combination of straight-road segments, bends, and different road slopes. During these trials, a tuning refinement was applied to the controllers because of the complexity of the translation from simulation to the real world.

To compare the two controllers in conditions as equal as possible, a predefined route was recorded. This route was first traveled over with the manually driven vehicle, and all the relevant variables to perform the control—position, speed and acceleration—were stored. In this way, the human influence in two consecutive trials was removed. In a parallel line, a PI controller previously developed to perform this application [5] was used to compare the novel controllers with previous results.

Fig. 9. shows the results for each of the controllers—PI, i-PI, and fuzzy—during this experiment. The distance between vehicles at the beginning of the test was set at 6 metres. Once this distance was achieved with 1-cm accuracy using the RTK-DGPS positioning system, the test was initiated. The top plot depicts the trailing vehicle's speed with respect to the leading one. The second from the top shows the desired inter-distance and the values obtained using the designed controllers. The third shows the desired relative velocity and the values obtained by the controllers. The fourth and fifth show the acceleration and the jerk, respectively, for the three controllers. The bottom plot shows the action on the accelerator and brake pedals, with the values being normalized to the range $[-1, 1]$, where 1 indicates an action on the accelerator pedal and -1 on the brake.

At the beginning, the leading car is stopped at the predefined safety distance—6 m. During the first minute, the fuzzy

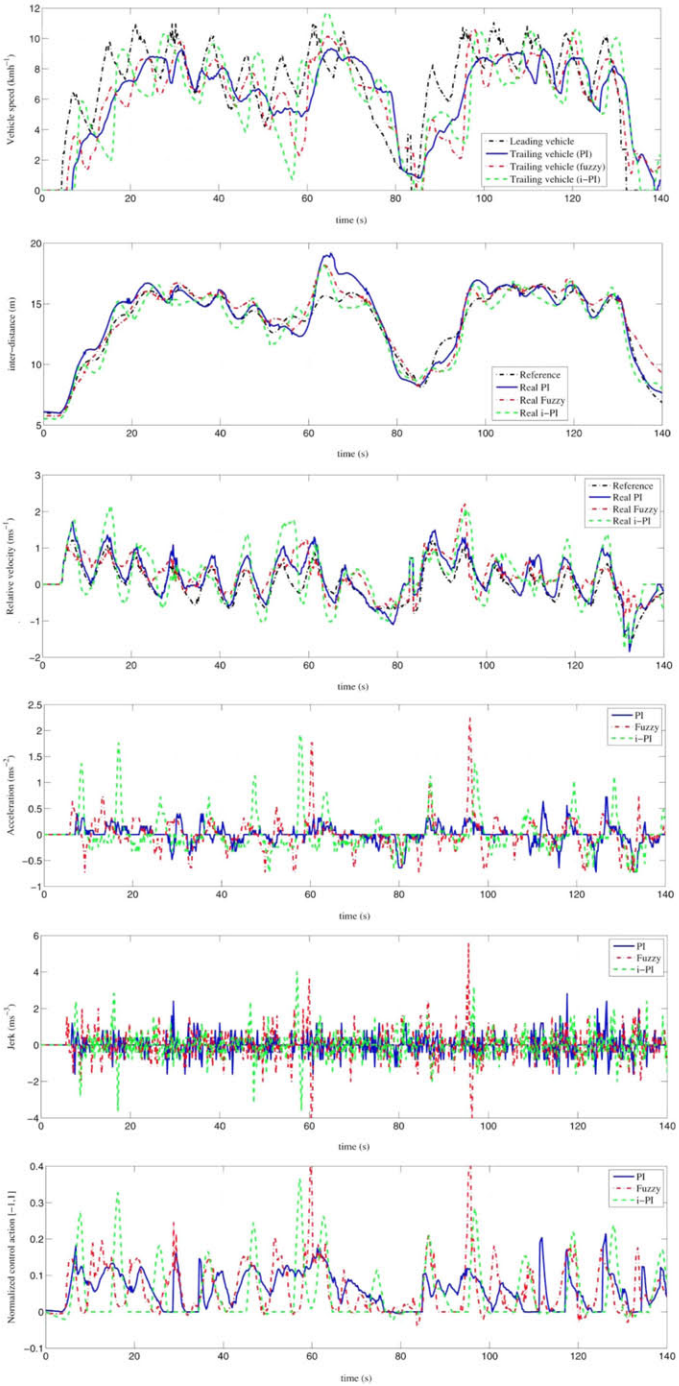

Fig. 9. (a) Leading and trailing vehicle speeds. (b) Distance between vehicles. (c) Relative velocity. (d) Acceleration. (e) Jerk. (f) Normalized control action.

controller is very close to the reference inter-distance and the i-PI controller is slightly under the desired value. One can appreciate how the PI controller presents the poorest behavior with greater values than the reference inter-distance. This behavior is reflected in the desired relative velocity. The greatest inter-distance error occurs at around second 64, because the autonomous vehicle is driving around a curved stretch. Then, at around second 85, the leading car's speed is significantly slowed to close to zero at the end of a straight stretch. When the leading vehicle starts again, a minimal delay appears in the fuzzy controller that is resolved with hard action on the throttle to recover the desired inter-distance. Later, the fuzzy controller follows the reference with better precision than the i-PI up to second 130 when the leading car is stopped. Then, the i-PI controller reaches the predefined safety distance faster than the fuzzy controller. Variations in the PI controller are greater than the other two controllers throughout the test.

TABLE VI
EXPERIMENTATION PERFORMANCE CRITERIA

IAE	PI	i-PI	Fuzzy
e_p	0.587	0.351	0.315
e_v	0.283	0.3294	0.277
u_s	0.0112	0.0079	0.0137
J	0.8812	0.6883	0.6057

Concerning the acceleration and jerk, all three controllers satisfied the initial prerequisites—$\gamma_{\max} = 2$ ms^{-2}, $J_{\max} = 5$ ms^{-3}. With respect to the control action, the smoothest is attained by the i-PI controller. The fuzzy controller presents the greatest oscillations in control actions, but they can be neglected from a perspective of the comfort of the car's occupants.

To quantify these results, the control quality indicators introduced in Section III-C1 are compared in Table VI. One observes that the tracking error is better in the fuzzy than in the i-PI controller, but that the control action is harsher in the fuzzy controller.

In brief therefore, the fuzzy controller presents as its main advantage that it can be intuitively retuned and behaves slightly better in tracking, the i-PI controller has smoother control action, and the PI controller presents the poorest behavior of the three.

Remark 2: There are numerous effects that appear in real experiments that are extremely difficult to quantify (weather conditions, the pavement of the road, pressure on the wheel, etc.). Thus, although the i-PI controller worked better in our simulations, the fuzzy controller parameters were less sensitive than those of the i-PI when translated to the real world.

V. CONCLUSION

Stop-and-go manœuvres constitute one of the most important and as yet unsolved topics in the automotive sector. This paper has presented two control techniques—fuzzy logic and i-PI controllers—with which to solve this problem. First, a car model was used to validate the proposed controllers. Then, two real cars were used to check the behaviour of the control algorithm in real circumstances. The following lessons can be learned from this work.

- The fuzzy controller developed can be easily adapted from simulations to the real word since it is based on human behavior and is a model-free control technique.
- The i-PI controller, that it is only based on a rough model of the system, provides smoother action on the throttle and brake pedals, thus increasing the vehicle occupants' comfort.
- The behavior of both these new controllers is significantly better than a controller developed previously [5] to perform this manoeuvre.
- The proposed control techniques can significantly reduce traffic jams, making driving easier by relieving the human driver of some tedious tasks.

The promising results obtained with the two controllers in the work described in this paper will be pursued analytically and experimentally with more vehicles and in other advanced driver assistance systems.

REFERENCES

[1] A. Kestinga, M. Treibera, M. Schönhofa, and D. Helbing, "Adaptive cruise control design for active congestion avoidance," *Transportation Res. Pt. C, Emerging Technol.*, vol. 16, no. 6, pp. 668–683, Dec. 2008.

[2] B. van Arem, C. J. G. van Driel, and R. Visser, "The impact of cooperative adaptive cruise control on traffic-flow characteristics," *IEEE Trans. Intell. Transportation Syst.*, vol. 7, no. 4, pp. 429–436, 2006.

[3] N. B. Hounsell, B. P. Shrestha, J. Piao, and M. McDonald, "Review of urban traffic management and the impacts of new vehicle technologies," *IET Intell. Transport Syst.*, vol. 3, no. 4, pp. 419–428, 2009.

[4] S. Moon, I. Moon, and K. Yi, "Design, tuning and evaluation of a full-range adaptive cruise control system with collision avoidance," *Control Eng. Pract.*, vol. 17, pp. 442–455, 2009.

[5] J. Martinez and C. C. de Wit, "A safe longitudinal control for adaptive cruise control and stop-and-go scenarios," *IEEE Trans. Control Syst. Technol.*, vol. 15, no. 1, pp. 246–258, Jan. 2007.

[6] D. Swaroop, J. Hedrick, C. Chien, and P. Ioannou, "A comparision of spacing and headway control laws for automatically controlled vehicles 1," *Veh. Syst. Dyn.*, vol. 23, no. 1, pp. 597–625, 1994.

[7] J. Naranjo, C. González, R. Garcia, and T. de Pedro, "ACC+ Stop&go maneuvers with throttle and brake fuzzy control," *IEEE Trans. Intell. Transportation Syst.*, vol. 7, no. 2, pp. 213–225, Jun. 2006.

[8] S. Dermann and R. Isermann, "Nonlinear distance and cruise control for passenger cars," in *Proc. Amer. Control Conf.*, 1995, pp. 3081–3085.

[9] J. Gerdes and J. Hedrick, "Vehicle speed and spacing control via coordinated throttle and brake actuation," *Control Eng. Pract.*, vol. 5, no. 11, pp. 1607–1614, 1997.

[10] L. Nouveliere and S. Mammar, "Experimental vehicle longitudinal control using a second order sliding mode technique," *Control Eng. Pract.*, vol. 15, no. 8, pp. 943–954, 2007.

[11] H. Raza, Z. Xu, B. Yang, and P. Ioannou, "Modeling and control design for a computer-controlled brake system," *IEEE Trans. Control Syst. Technol.*, vol. 5, no. 3, pp. 279–296, Sep. 1997.

[12] K. Yi and J. Chung, "Nonlinear brake control for vehicle CW/CA systems," *IEEE/ASME Trans. Mechatron.*, vol. 6, no. 1, pp. 17–25, Jan. 2001.

[13] Y. Dote and S. J. Ovaska, "Industrial applications of soft computing: A review," *Proc. IEEE*, vol. 89, no. 9, pp. 1243–1265, Sep. 2001.

[14] L. Zadeh, "Fuzzy sets," *Inf. Control*, vol. 8, pp. 338–353, 1965.

[15] M. Sugeno and M. Nishida, "Fuzzy control of a model car," *Fuzzy Sets Syst.*, vol. 16, no. 2, pp. 103–113, 1985.

[16] M. Fliess and J. C. , "Intelligent PID controllers," in *Proc. 16th Mediterranean Conf. Control Autom.*, 2008, pp. 326–331.

[17] M. Fliess and C. Join, "Model-free control and intelligent PID controllers: Towards a possible trivialization of nonlinear control?," presented at the 15th IFAC Symp. Syst. Identification (SYSID), Saint-Malo, France, 2009.

[18] R. Rajamani, *Vehicle Dynamics and Control.*. New York: Springer, 2005.

[19] H. Pacejka and E. Bakker, "The magic formula tyre model," *Veh. Syst. Dyn.*, vol. 21, pp. 1–18, 2004.

[20] K. Aström and T. Hägglund, "Advanced PID Controllers," *Instrument Soc. Amer.*, 2006, TJ 223.P55A85.

[21] V. Milanés, E. Onieva, J. Pérez, T. de Pedro, and C. González, "Control de velocidad adaptativo para entornos urbanos congestionados," *Revista Iberoamericana Autom. Inf. Ind.*, vol. 6, no. 4, pp. 66–73, Oct. 2009.

[22] M. Sugeno and M. Nishida, "Fuzzy control of model car," *Fuzzy Sets Syst.*, vol. 16, pp. 103–113, 1985.

[23] J. Villagra, V. Milanés, J. Pérez, and T. de Pedro, "Control basado en PID inteligentes: Aplicación al control robusto de velocidad en entornos urbanos," *Revista Iberoamericana Autom. Inf. Ind.*, vol. 7, no. 4, pp. 44–52, Oct. 2010.

[24] R. Bourdais, M. Fliess, C. Join, and W. Perruquetti, "Towards a model-free output tracking of switched nonlinear systems," presented at the IFAC Symp. Nonlinear Control Syst., Pretoria, South Africa, 2007.

[25] V. Milanés, J. Villagrá, J. Pérez, and C. González, "Low-speed longitudinal controllers for mass-produced cars: A comparative study," *IEEE Trans. Ind. Electron.*, to be published.

[26] J. Pérez, C. González, V. Milanés, E. Onieva, J. Godoy, and T. de Pedro, "Modularity, adaptability and evolution in the AUTOPIA architecture for control of autonomous vehicles," in *Proc. IEEE Int. Conf. Mechatron. (ICM)*, 2009, pp. 1–5.

[27] V. Milanés, D. Llorca, B. Vinagre, C. González, and M. Sotelo, "Clavileño: Evolution of an autonomous car," in *Proc. 13th Int. IEEE Conf. Intell. Transportation Syst.*, 2010, pp. 1129–1134.

[28] V. Milanés, C. González, J. Naranjo, E. Onieva, and T. De Pedro, "Electro-hydraulic braking system for autonomous vehicles," *Int. J. Autom. Technol.*, vol. 1, no. 11, pp. 89–95, Feb. 2010.

[29] V. Milanés, J. E. Naranjo, C. Gonzalez, J. Alonso, and T. de Pedro, "Autonomous vehicle based in cooperative gps and inertial systems," *Robotica*, vol. 26, pp. 627–633, 2008.

[30] V. Milanés, J. Godoy, J. Pérez, B. Vinagre, C. González, E. Onieva, and A. J. , "V2I-based architecture for information exchange among vehicles," presented at the 7th Symp. Intell. Autonomous Veh., Lecce, Italy, 2010.